

Developing compact tuning fork thermometers for sub-mK temperatures and high magnetic fields

Cite as: J. Appl. Phys. **133**, 024501 (2023); <https://doi.org/10.1063/5.0132492>

Submitted: 28 October 2022 • Accepted: 22 December 2022 • Published Online: 13 January 2023

 A. J. Woods,  A. M. Donald,  R. Gazizulin, et al.



View Online



Export Citation



CrossMark

ARTICLES YOU MAY BE INTERESTED IN

[Synchronous electro-optical method for studying mixed ionic–electronic conductors with hopping transport](#)

Journal of Applied Physics **133**, 024901 (2023); <https://doi.org/10.1063/5.0120907>

[Domain wall chirality reversal by interfacial engineering in Pt/Co/Pt based perpendicularly magnetized systems](#)

Journal of Applied Physics **133**, 023907 (2023); <https://doi.org/10.1063/5.0117198>

[Temperature sensing with RF-dressed states of nitrogen-vacancy centers in diamond](#)

Journal of Applied Physics **133**, 024401 (2023); <https://doi.org/10.1063/5.0129706>



Time to get excited.
Lock-in Amplifiers – from DC to 8.5 GHz

[Find out more](#)

 Zurich
Instruments

Developing compact tuning fork thermometers for sub-mK temperatures and high magnetic fields

Cite as: J. Appl. Phys. **133**, 024501 (2023); doi: [10.1063/5.0132492](https://doi.org/10.1063/5.0132492)

Submitted: 28 October 2022 · Accepted: 22 December 2022 ·

Published Online: 13 January 2023



View Online



Export Citation



CrossMark

A. J. Woods,^{1,a)} A. M. Donald,¹ R. Gazizulin,¹ E. Collin,² and L. Steinke^{1,b)}

AFFILIATIONS

¹Department of Physics and National High Magnetic Field Laboratory High B/T Facility, University of Florida, Gainesville, Florida 32611-8440, USA

²CNRS, Institut Néel, Université Grenoble Alpes, 25 rue des Martyrs, 28042 Grenoble Cedex 9, France

^{a)}**Current address:** MPA-Q, Mailstop K764, Los Alamos National Laboratory, Los Alamos, New Mexico 87545, USA. **Author to whom correspondence should be addressed:** ajwoods@lanl.gov

^{b)}**Electronic mail:** lucia.steinke@ufl.edu

ABSTRACT

There is a growing demand for experiments on calorimetric and thermal transport measurements at ultra-low temperatures below 1 mK and high magnetic fields up to 16 T. Particularly, milligram-sized solid samples are of great interest. We present the development of scalable thermometers based on quartz tuning fork resonators immersed in liquid ³He and adapt hydrodynamic models to provide an improved description of temperature dependence in the high viscosity regime between 1 and 10 mK. We demonstrate successful thermometer operation and discuss the feasibility of fast and compact thermal probes suitable for small samples.

Published under an exclusive license by AIP Publishing. <https://doi.org/10.1063/5.0132492>

I. INTRODUCTION

The National High Magnetic Field Laboratory (NHMFL) High B/T facility at the University of Florida in Gainesville pursues the mission to enable user experiments at the combined extremes of high magnetic fields (high B) and ultra-low temperatures (ULT) below 1 mK. While almost all measurement techniques like electrical transport or magnetometry require adaptations to be successfully performed in this environment, calorimetry and thermal transport are particularly challenging due to a lack of suitable thermometry. High-resolution thermal measurements in this regime would be of great benefit to the study of exotic Fermi surfaces via quantum oscillations.^{1,2} Calorimetric measurements of quantum spin liquid (QSL) candidates could observe gapless excitations down to ultra-low temperatures, which would be important to demonstrate a QSL ground state.³ Furthermore, thermal transport is a key experimental probe for the nodal structure of superconductors,⁴⁻⁶ and improved ULT thermometry could allow for studies of superconductors with extremely low transition temperatures such as bismuth,⁷ as well as revealing characteristics of topologically non-trivial systems via the thermal Hall effect.^{8,9}

Motivated by these experimental challenges, we seek to develop thermometers that are suitable for measurements of

typically milligram sized solid samples and are compatible with environments below 1 mK and high magnetic fields of 16 T and beyond. Existing thermometry options typically have at least one drawback that makes them unsuitable for these combined goals. Resistive thermometry has a minimum temperature of around 20 mK,¹⁰ and SQUID noise thermometers are incompatible with high magnetic fields.^{11,12} ³He melting curve thermometry¹³ and nuclear magnetic resonance thermometers¹⁴ have too high masses and long thermalization times to allow for measurements of small samples. Coulomb blockade thermometers show promise as ultra-low temperature thermometers,¹⁵⁻¹⁸ but typically require delicate on-lead magnetic demagnetization stages or on-chip cooling, which makes them incompatible or too complicated to use as sample thermometers in high magnetic fields.

Here, we investigate quartz tuning fork thermometry in liquid ³He, which could potentially meet all of the experimental requirements of low thermal masses, sensitivity to ULT, and compatibility with high magnetic fields. The measurement principle relies on the temperature dependent viscosity of liquid ³He that is probed by tracking the resonance of quartz tuning forks immersed in the liquid. First, quartz tuning forks are widely used in studies of the ULT properties of the helium liquids¹⁹⁻²⁷ with a minimum

temperature of $100\ \mu\text{K}$ in ^3He ; therefore, their compatibility with a ULT environment is well established. Second, thermometers tracking the vacuum resonance of a tuning fork have been used at intermediate magnetic fields up to 8 T,²⁸ and magnetometers based on tuning forks in ^4He exchange gas have even been successfully operated at high magnetic fields up to 64 T and at temperatures around 1.3 K.^{29,30} Third, since the tuning forks measure viscosity—an intrinsic property of the ^3He liquid—the thermometer signal does not depend on its mass, allowing for miniaturized temperature probes for studies on small solid samples.

We report on first measurements that subject quartz tuning fork thermometers (TFTs) filled with liquid ^3He to the combined extremes of ultra-low temperatures down to 1 mK and high magnetic fields up to 14.5 T. We measure in the regime above the superfluid transition, where the viscosity of helium 3 is so high that simple hydrodynamic models^{24,25} fail to predict the tuning fork resonance characteristics, and where the tuning forks require large driving forces which may affect the field dependence. In this work, we attempt an adaptation of existing hydrodynamic models that take into account slip in the high viscosity regime based on previous treatments for different vibrating object geometries modified with empirical fit parameters.^{31–33} We also revisit the idea²⁴ that even without observing the fixed point at the superfluid transition, TFTs in liquid ^3He may provide almost-primary thermometry with a predictable temperature dependence and require minimal or no calibration. We argue that the geometry-dependent crossover to the slip-corrected regime could serve as an alternative fixed point. Finally, we discuss recent progress in miniaturization of TFTs and establish current resolution limits for thermal measurements based on prototype dimensions and the resolution obtained in the experiments presented here.

II. TUNING FORK THERMOMETRY AT ULTRA-LOW TEMPERATURE AND HIGH MAGNETIC FIELD

We first establish the vacuum properties of the Lorentzian tuning fork resonances, then discuss the temperature dependent damping due to the viscosity of the normal fluid ^3He . We go on to compare the temperature dependence of the resonance properties to prediction of two hydrodynamic models. We also verify that the tuning forks are insensitive to magnetic fields even when immersed in highly viscous liquid ^3He , where comparatively large drive amplitudes are required.

A. Tuning fork vacuum properties

Quartz tuning forks are piezoelectric resonators and are characterized by the tuning fork constant a , which is used to determine the velocity response to an applied driving force. a depends only on the properties of the quartz and the tuning fork dimensions, the tine length, \mathcal{L} , the tine thickness, \mathcal{T} and the tine width, \mathcal{W} . The tuning forks we use here are the Epson C-002RX, a commercially available device, hereafter referred to as CTF, and a tuning fork from an array manufactured by Statek corporation for use in previous work on quantum turbulence in superfluid ^3He .³⁴ We chose the tuning fork that showed the strongest response in vacuum testing from this array, labeled ATF5. The tuning forks are shown

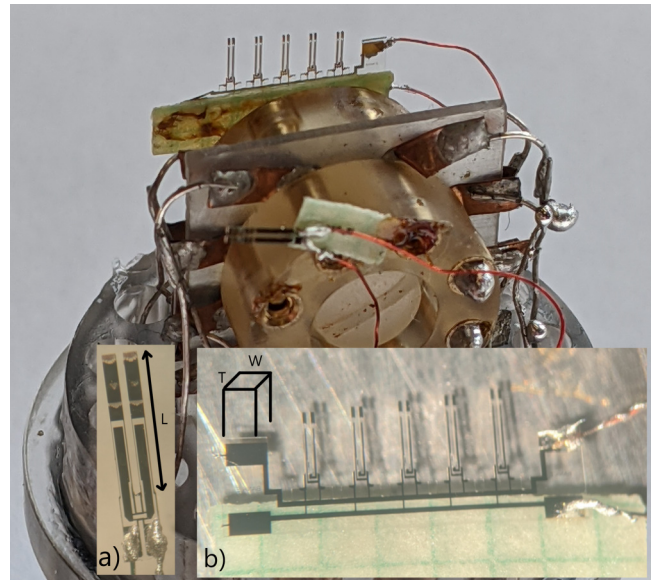


FIG. 1. The polycarbonate cell insert used in this work, showing the CTF (front) and Array of tuning forks (back). Inset: the tuning forks studied in this work. (a) An Epson C-002RX commercial tuning fork (CTF), nominal resonance frequency 32.768 kHz. (b) An array of five tuning forks, provided by Viktor Tsepelin, Lancaster University, UK.³⁴

in the inset of Fig. 1 and their physical dimensions are summarized in Table I.

To use the tuning forks as thermometers, the vacuum resonance frequency and width need to be known. We, therefore, took care to measure the properties in vacuum at $T \leq 1.5$ K. This temperature was chosen to minimize the residual vapor pressure in the cell and to eliminate the temperature dependence of the quartz properties.²⁴ The tuning fork constant a is derived from the properties of the vacuum resonance and is given by

$$a = \sqrt{\frac{4\pi m_e I_0 \Delta f}{V_0}}, \quad (1)$$

where I_0 is the response current peak amplitude, V_0 is the driving voltage amplitude, Δf is the width of the Lorentzian resonance, and $m_e = 0.25\rho_q \mathcal{L}\mathcal{W}\mathcal{T}$ is the effective mass of a tuning fork tine. Further details are given in the [supplementary material](#). The vacuum properties of the tuning forks are summarized in Table I.

TABLE I. Summary of the dimensions of the tuning forks used in this work.

| Tuning fork | \mathcal{L} (μm) | \mathcal{T} (μm) | \mathcal{W} (μm) | a (C m^{-1}) | Δf_{vac} (Hz) |
|-------------|---------------------------------|---------------------------------|---------------------------------|---------------------------|------------------------------|
| CTF | 3000 | 230 | 100 | 2.78×10^{-6} | 0.110 |
| ATF5 | 1450 | 90 | 75 | 8.42×10^{-7} | 0.070 |

TABLE II. A summary of the resonant widths of each tuning fork for different temperatures in normal fluid ^3He .

| Temperature (mK) | CTF Δf (Hz) | ATF5 Δf (Hz) |
|------------------|---------------------|----------------------|
| 100 | 40 | 90 |
| 30 | 120 | 300 |
| 10 | 410 | 950 |
| 5 | 1065 | 1600 |

The measured width for the ATF5 is consistent with the ULT (2 mK) width measured previously for a similar fork.²⁰

B. Temperature dependence

Characterization of the tuning forks in bulk ^3He was performed in the Bay 3 cryostat at the NHMFL High B/T Facility, at 0 bar in a liquid ^3He cell cooled by a PrNi₅/Cu hybrid nuclear demagnetization stage. The base temperature of this cryostat is around 700 μK , and primary thermometry was provided by a ^3He melting curve thermometer (MCT).¹³ The tuning fork resonances were continuously monitored as the temperature was changed in the range 1–100 mK by magnetizing and demagnetizing the nuclear stage. Magnetic field was applied along the cylindrical axis of the cell such that the field was along the length of the tuning fork tines for ATF5 and normal to the tines for the CTF.

Figure 2(a) shows the measured resonance curves for the CTF, for three different temperatures in liquid ^3He . The widths obtained from Lorentzian fits to the resonance curves depend strongly on the temperature dependent viscosity of the ^3He , as shown in Fig. 2(b) and summarized in Table II. We calculated the expected T -dependence using an equation for the resonance width of the tuning fork Δf in terms of the viscosity η of the ^3He derived in Blaauwgeers *et al.*,²⁴

$$\Delta f = \frac{1}{2} \sqrt{\frac{\rho \eta f_0}{\pi}} C S \frac{(f_0/f_{vac})^2}{m_e}, \quad (2)$$

where C is a geometric constant of order unity, which typically has a value around 0.6 for tuning forks of the type used here.²⁵ $S = 2\mathcal{L}(\mathcal{T} + \mathcal{W})$ is the surface area of the tuning fork tines, and m_e is the effective mass of a tuning fork tine. f_0 and f_{vac} are the resonant frequency and vacuum resonant frequency, respectively. The temperature dependence of the viscosity of ^3He is well established³⁵ as $\eta \propto T^{-2}$. We, therefore, expect a T^{-1} dependence of the width [dashed lines in Fig. 2(b)]. At $T > 20$ mK, the CTF deviates from the expected temperature dependence which we attribute to poor thermalization during a relatively rapid cooldown, resulting in the temperature of the MCT being lower than the temperature of the cell.

Below 5 mK for the CTF and 7 mK for ATF5, despite sufficient thermalization times, both tuning forks deviate from T^{-1} . This shows the limitation of the simple model developed by Blaauwgeers *et al.*, which considers the effects of two flow fields: potential flow far away from the tuning fork tines and rotational flow near the tines, leading to an enhancement of the effective mass. This model

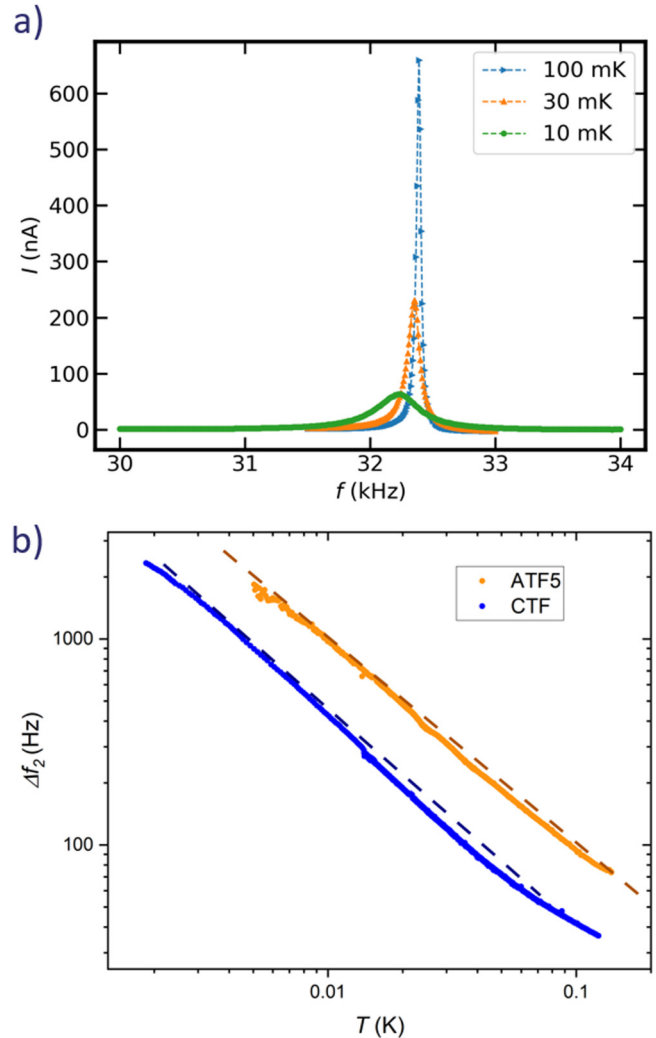


FIG. 2. (a) Resonance curves (response current as a function of frequency) at a constant driving force for the CTF. (b) Resonance width as a function of temperature for CTF and ATF5, the dashed lines are guides to the eye for T^{-1} .

yields a good prediction of the temperature dependence of the tuning fork width, if the viscous penetration depth δ , where

$$\delta = \sqrt{\frac{\eta}{\rho \pi f}}, \quad (3)$$

which is a measure of the extent of the flow field, is small enough that the flow fields do not interfere, which is the case as long as δ is much smaller than the relevant tuning fork dimension. At the lowest temperatures studied here, this condition is no longer fulfilled, and we observe deviation from the model prediction. We label this regime the high viscosity limit and attempt an advanced hydrodynamic description in Sec. II C.

C. Slip correction

At high viscosity, the liquid is no longer able to follow the motion of the vibrating object immersed in it. Instead, a non-zero velocity, or slip, occurs at the surface of the tuning fork tines. After the onset of slip, the flow fields grow more slowly with increasing viscosity and the role of interfering flow fields may be diminished. In the following, we discuss a semi-empirical hydrodynamic model accounting for the effects of surface slip in tuning forks by adapting models developed to include slip corrections for vibrating objects of different geometries. This provides an improved fit to experimental data and allows for the prediction of some low temperature characteristics. We combine the hydrodynamic models derived by Zhang *et al.*,³³ Brumley *et al.*,³¹ and Jensen *et al.*³²

Zhang *et al.*³³ describe the properties of the tuning fork in terms of hydrodynamic functions. In this model, the resonant frequency of the first vibrational mode of a quartz tuning fork is

$$(2\pi f_0)^2 = (2\pi f_1)^2 \left(1 + \frac{\pi \mathcal{W}}{4\rho_q \mathcal{T}} \rho \Gamma_{hydro}^r (2\pi f_1) \right), \quad (4)$$

and the quality factor of that mode is

$$Q_1 = \frac{2\pi f_1}{2\pi \Delta f_1} = \frac{\frac{4\rho_q e}{\pi p l} + \Gamma_{hydro}^r}{\Gamma_{hydro}^i}, \quad (5)$$

where $2\pi f_0$ is the resonant frequency in vacuum and \mathcal{W} and \mathcal{T} are the width and thickness of the tuning fork tines, respectively. ρ_q is the density of quartz, ρ is the fluid density, and Γ_{hydro}^r and Γ_{hydro}^i are the real and imaginary parts of the hydrodynamic function taken from tabulated values.³¹

Using the above expression derived in the absence of slip, we apply the slip correction developed by Jensen *et al.*,³² modifying the hydrodynamic function as follows:

$$\Gamma(2\pi f) - 1 = \frac{1}{\frac{1}{\Gamma_0(2\pi f) - 1} - i \left(\frac{T/2}{\sqrt{2}\delta} \right) \left(\frac{l_{slip}}{l_{slip} + T/2} \right)}, \quad (6)$$

where $\Gamma_0(2\pi f)$ is the hydrodynamic function without slip correction, $l_{slip} = const \left(\frac{1+\sigma}{1-\sigma} \right) l_{mfp}$ and δ is the viscous penetration depth. σ is the specularity of the surface of the tuning fork, and l_{mfp} is the mean free path in the fluid.

We apply the modified hydrodynamic model to improve the description of the temperature dependent resonance properties of three different tuning forks. Figure 3(a) shows the width of the ATF5, CTF, and a third tuning fork, measured previously in Grenoble, and referred to as GTF resonances as a function of temperature in the range 20–1 mK. The dashed lines show the result of the calculation of the slip corrected tuning fork width. We allow the specularity, σ , to vary as a fork-dependent, but temperature-independent fitting parameter, which is likely related to the details of the tuning fork surface.

We observe that the slip correction becomes necessary at temperatures $T \leq T_s$, where T_s is the temperature at which $\delta = \mathcal{W}/3$, as shown in Fig. 3(b). This limit is consistent with that observed

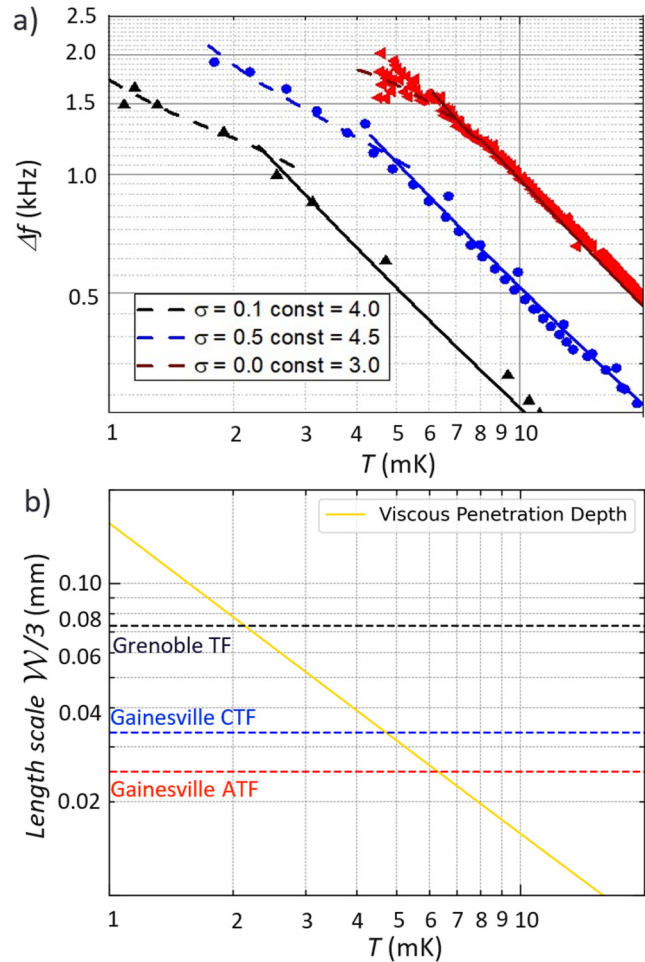


FIG. 3. (a) The resonance width as a function of nuclear stage temperature for GTF (black), CTF (blue), and ATF5 (red). The solid lines are calculated values of the width using hydrodynamic functions from Brumley *et al.*,³¹ the dashed lines are a slip correction³² where the specularity, σ , and slip length coefficient *const* are fit parameters. (b) A plot showing the tuning fork length scale vs temperature. The solid line shows the viscous penetration depth, and the dotted lines the values of $W/3$ for each tuning fork measured here.

for slip in a vibrating wire resonator.³⁶ We conclude that the deviation from the simple model is indeed due to slip and suggest that this crossover could be used as a fixed point for calibrating these thermometers as the temperature where it occurs is predicted by the tuning fork geometry.

D. High field tests

To establish the suitability of TFTS at high B and ULT, we performed two sets of tests: field sweeps near 18 mK, the base temperature of the dilution refrigerator and demagnetization cool-downs at fixed high field.

Figure 4(a) shows the width of ATF5 as a function of the applied magnetic field. The width changes as the field is changed and relaxes while the field remains constant. We attribute this to eddy current heating in the silver cold finger that links the nuclear stage to the ^3He cell, causing heating of the ^3He in the cell, consistent with the temperature measured independently by the MCT [Fig. 4(b)]. Figure 4(c) shows the tuning fork constant, a , as a function of the applied field. a is determined from Eq. (1) using fit parameters extracted from fits to the Lorentzian resonance. While the tuning fork resonance shows a direct response to the temperature changes in the cell, the tuning fork constant remains within 0.6% of its $B = 0$ value even at the highest field of 14.5 T, confirming that there is no residual magnetic field dependence once the temperature changes are accounted for. This illustrates that ULT cannot be maintained during a magnetic field sweep; therefore, performance tests at ULT and high B are achieved by T -sweeping at a constant magnetic field.

Figure 4(d) shows the tuning fork constant, a , of the CTF as a function of temperature at 14.5 T (blue) and 0 T (orange) where the zero-field fork constant is derived from the data presented in Fig. 2(b). The fork constant in the applied magnetic field is again calculated using Eq. (1) and fits to the Lorentzian line shape measured during the cooldown. The CTF exhibits the same insensitivity to the applied magnetic field as the ATF5. This confirms that there is no significant magnetic field induced effect on the properties of

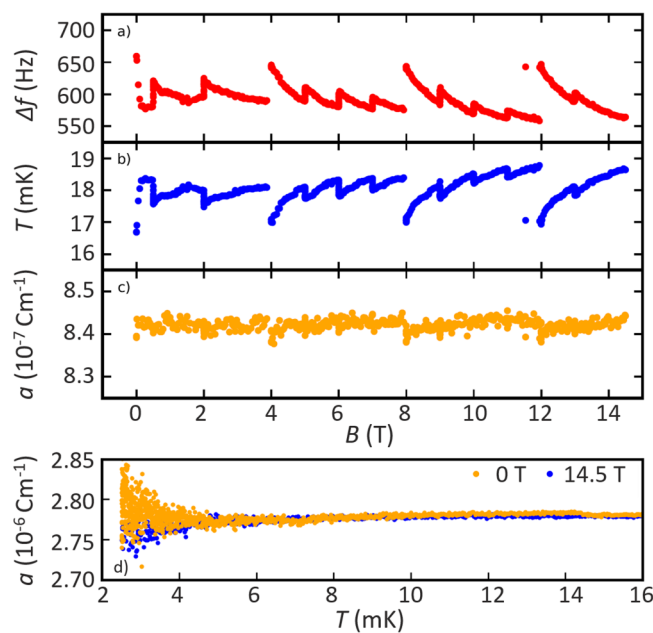


FIG. 4. (a) The resonance width of ATF5 as a function of the applied magnetic field during a sequence of field sweeps. (b) The temperature inferred from the melting curve thermometer during the same field sweeps. (c) The tuning fork constant, a , as calculated from the fitted resonance curve as a function of the applied field. (d) The tuning fork constant, a , as a function of temperature for the CTF, during two different demagnetizations at 14.5 T (blue) and 0 T (orange).

the quartz, the tuning fork electrodes, or on the viscosity of ^3He . The tuning forks are, therefore, suitable as thermometers in the temperature and magnetic field ranges of interest. The deviation of a below 5 mK results from the onset of slip, and further work is required to correct the tuning fork constant in this regime.

III. TUNING FORKS IN ^3He AS THERMAL PROBES FOR SMALL SAMPLES

Having established compatibility of the TFTS with high B and ULT, we discuss adaptations for the measurement of small solid samples. To probe such samples in specific heat and thermal transport measurements, the thermal mass of the thermometer must be small enough that temperature changes caused by the thermal response of the sample can be detected. A lower thermal mass also corresponds to a faster response time of the thermometer, which allows for measurements with higher resolution in a given time frame. This can be achieved by reducing the ^3He volume as much as possible, since the dominant contribution to the ULT specific heat of ^3He cells generally stems from the liquid itself.³⁵ As the tuning fork directly probes the viscosity of the surrounding liquid, its measurement signal is independent of the total ^3He mass. Therefore, reducing the amount of ^3He should not come at the expense of temperature resolution or alter the measurement result. However, if the tuning fork comes within the viscous penetration depth of the wall of the thermometer, additional adaptations to the hydrodynamic model will be required to correctly predict the temperature dependence. As the thermal mass of the thermometer is reduced, care should also be taken to maintain the tuning fork driving force and tine velocity at a low enough level that the tuning fork does not self heat the thermometer, or to run the tuning fork in pulses so as to reduce the time that the tuning fork can deposit heat into the thermometer.

Figure 5 shows prototype tuning fork thermometers that represent first attempts at minimizing the ^3He volume while still allowing for enough space for the tuning fork to ring freely, to add or remove ^3He via a fill capillary, and ensuring good thermal contact via an integrated heat exchanger. Tuning forks have previously been used in compact geometries for bolometry in superfluid ^3He -B³⁴ and for thermal transport in confined ^3He .²⁶ The key difference here is the complete enclosure with a heat exchanger and with the intention of mounting a small solid state sample for thermal measurements. Both prototypes contain nominally identical CTFs and silver heat exchangers and are sealed with epoxy plugs at either end. The thermometer in panel (a) is constructed from a high purity silver body and a schematic of the components inside is overlaid, (b) shows a variation on this design, with a silver wire directly pressed into the heat exchanger, to improve thermal contact with a sample mounted on the wire. We estimate the total specific heat of these thermometers to be around $4\mu\text{J}/\text{K}$ at 1 mK in zero applied magnetic field, based on the published values for ^3He ³⁵ and silver.³⁷ The magnetic field dependence of the heat capacity of the thermometer is to be determined in future prototypes. The thermalization time of the thermometer depends on the specific heat and the thermal resistance determined by the surface area of the silver heat exchanger.³⁸ For a heat exchanger of the size shown in Fig. 5(a), assuming a 50% packing fraction, we calculate

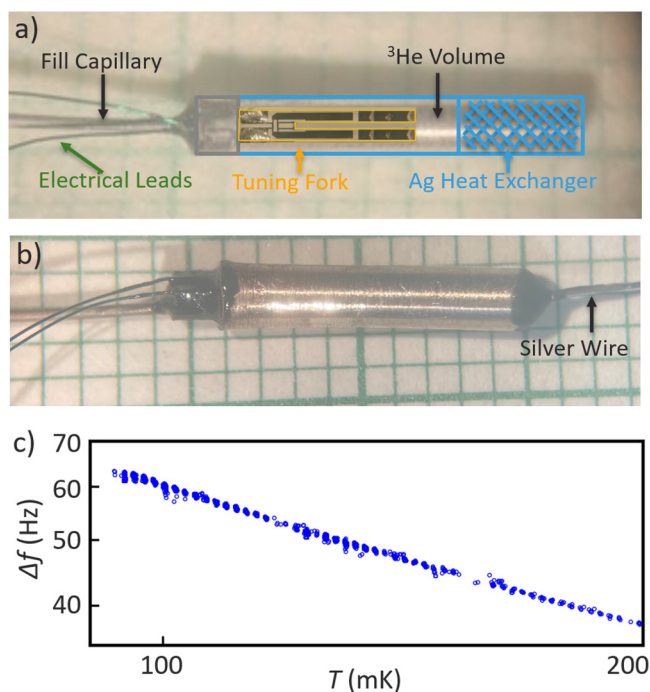


FIG. 5. Prototype tuning fork thermometers comprising a CTF and silver sinter heat exchanger encased in a silver tube. (a) Schematic overlay showing the internal components and dimensions, (b) a newer prototype, showing the silver wire for the thermal link to the sample. (c) The resonance width as a function of temperature for the TFT pictured in (b).

that the response time of the thermometer is of order 50 s, which is a comparably rapid response in the context of ULT experiments. Figure 5(c) shows the resonance width of the TFT pictured in Fig. 5(b) down to temperatures of around 90 mK, showing comparable temperature dependence to tuning forks in larger cells, which confirms adequate thermalization and establishes that mini TFTs of this design are leak tight and can be successfully filled by condensing ^3He . The next step is to test this thermometer and other prototypes down to 1 mK and in applied magnetic fields.

Based on the present accuracy of the temperature measurement based on the tuning fork width ($\approx 50\mu\text{K}$), we assume that the detection limit of the tuning fork thermometer is around 1% of its own specific heat, i.e., it should be capable of measuring samples with specific heat 40 nJ K^{-1} , comparable to the specific heat of small single crystal samples that users of the High B/T facility may want to investigate.

IV. SUMMARY

We have shown that quartz tuning forks immersed in liquid ^3He provide robust thermometry at the combined extremes of ultra-low temperatures down to 1 mK and high magnetic fields up to 14.5 T, presenting a viable platform for temperature measurements in this regime. We also presented an adaptation of

hydrodynamic models to improve temperature calibration in the high viscosity regime between 1 and 10 mK. We discussed the feasibility of miniature thermometers that could provide much needed thermal probes for user experiments on small solid state samples in the extreme environments accessible at the NHMFL High B/T Facility. Existing thermometer prototypes built with relatively simple fabrication methods could already be suitable for a large number of measurements extending the typical temperature range for thermal measurements below $\sim 20\text{ mK}$.

SUPPLEMENTARY MATERIAL

See the [supplementary material](#) for a description of the preparation of the tuning forks, details of the tuning fork measurement circuit, and a more complete derivation of the equations that govern the tuning fork motion.

ACKNOWLEDGMENTS

Experiments were performed at the National High Magnetic Field Laboratory (NHMFL) High B/T Facility at the University of Florida and at Université Grenoble Alpes CNRS. The NHMFL is supported by the National Science Foundation Cooperative Agreement (No. DMR-1644779) and the State of Florida. The authors also acknowledge support from the NHMFL User Collaboration Grants Program (UCGP). The Grenoble ULT Group has received funding from the European Union's Horizon 2020 Research and Innovation Programme under Grant Agreement No. 824109, the European Microkelvin Platform (EMP). The quartz tuning fork array was provided by Viktor Tsepelin, Lancaster University, UK. The authors also thank Viktor Tsepelin for useful discussions.

AUTHOR DECLARATIONS

Conflict of Interest

The authors have no conflicts to disclose.

Author Contributions

A. J. Woods: Conceptualization (equal); Formal analysis (equal); Investigation (equal); Methodology (equal); Software (equal); Writing – original draft (equal); Writing – review & editing (equal). **A. M. Donald:** Investigation (equal); Software (equal); Visualization (equal). **R. Gazizulin:** Data curation (equal); Investigation (equal); Visualization (equal); Writing – review & editing (equal). **E. Collin:** Investigation (equal); Writing – review & editing (equal). **L. Steinke:** Data curation (equal); Formal analysis (equal); Funding acquisition (equal); Investigation (equal); Methodology (equal); Supervision (equal); Visualization (equal); Writing – original draft (equal); Writing – review & editing (equal).

DATA AVAILABILITY

The data that support the findings of this study are available from the corresponding author upon reasonable request.

REFERENCES

- ¹B. S. Tan, Y.-T. Hsu, B. Zeng, M. C. Hatnean, N. Harrison, Z. Zhu, M. Hartstein, M. Kiourlappou, A. Srivastava, M. D. Johannes, T. P. Murphy, J.-H. Park, L. Balicas, G. G. Lonzarich, G. Balakrishnan, and S. E. Sebastian, "Unconventional Fermi surface in an insulating state," *Science* **349**, 287–290 (2015).
- ²D. Aoki, H. Sakai, P. Opletal, Y. Tokiwa, J. Ishizuka, Y. Yanase, H. Harima, A. Nakamura, D. Li, Y. Homma, Y. Shimizu, G. Knebel, J. Flouquet, and Y. Haga, "First observation of the de Haas–Van alphen effect and Fermi surfaces in the unconventional superconductor UTe_2 ," *J. Phys. Soc. Jpn.* **91**, 083704 (2022).
- ³C. Broholm, R. J. Cava, S. A. Kivelson, D. G. Nocera, M. R. Norman, and T. Senthil, "Quantum spin liquids," *Science* **367**, eaay0668 (2020).
- ⁴Y. Matsuda, K. Izawa, and I. Vekhter, "Nodal structure of unconventional superconductors probed by angle resolved thermal transport measurements," *J. Phys.: Condens. Matter* **18**, R705–R752 (2006).
- ⁵M. Sutherland, J. Dunn, W. H. Toews, E. O'Farrell, J. Analytis, I. Fisher, and R. W. Hill, "Low-energy quasiparticles probed by heat transport in the iron-based superconductor $LaFePO_4$," *Phys. Rev. B* **85**, 014517 (2012).
- ⁶T. Metz, S. Bae, S. Ran, I.-L. Liu, Y. S. Eo, W. T. Fuhrman, D. F. Agterberg, S. M. Anlage, N. P. Butch, and J. Paglione, "Point-node gap structure of the spin-triplet superconductor UTe_2 ," *Phys. Rev. B* **100**, 220504 (2019).
- ⁷O. Prakash, A. Kumar, A. Thamizhavel, and S. Ramakrishnan, "Evidence for bulk superconductivity in pure bismuth single crystals at ambient pressure," *Science* **355**, 52–55 (2016).
- ⁸M. Kawano and C. Hotta, "Thermal Hall effect and topological edge states in a square-lattice antiferromagnet," *Phys. Rev. B* **99**, 054422 (2019).
- ⁹X.-T. Zhang, Y. H. Gao, C. Liu, and G. Chen, "Topological thermal Hall effect of magnetic monopoles in the pyrochlore $U(1)$ spin liquid," *Phys. Rev. Res.* **2**, 013066 (2020).
- ¹⁰S. S. Courts, J. K. Krause, J. G. Weisend, J. Barclay, S. Breon, J. Demko, M. DiPirro, J. P. Kelley, P. Kittel, A. Klebaner, A. Zeller, M. Zagarola, S. V. Sciver, A. Rowe, J. Pfothenauer, T. Peterson, and J. Lock, "A commercial ruthenium oxide thermometer for use to 20 milliKelvin," *AIP Conf. Proc.* **985**, 947 (2008).
- ¹¹D. Rothfuss, A. Reiser, A. Fleischmann, and C. Enss, "Noise thermometry at ultra-low temperatures," *Philos. Trans. R. Soc. A: Math., Phys. Eng. Sci.* **374**, 20150051 (2016).
- ¹²A. Kirste and J. Engert, "A SQUID-based primary noise thermometer for low-temperature metrology," *Philos. Trans. R. Soc. A: Math., Phys. Eng. Sci.* **374**, 20150050 (2016).
- ¹³W. Ni, J. S. Xia, E. D. Adams, P. S. Haskins, and J. E. McKisson, " ^3He melting pressure temperature scale below 25 mK," *J. Low Temp. Phys.* **99**, 167–182 (1995).
- ¹⁴R. Tycko, "NMR at low and ultralow temperatures," *Acc. Chem. Res.* **46**, 1923–1932 (2013).
- ¹⁵J. P. Pekola, J. J. Toppari, J. P. Kauppinen, K. M. Kinnunen, A. J. Manninen, and A. G. M. Jansen, "Coulomb blockade-based nanothermometry in strong magnetic fields," *J. Appl. Phys.* **83**, 5582–5584 (1998).
- ¹⁶L. Casparis, M. Meschke, D. Maradan, A. C. Clark, C. P. Scheller, K. K. Schwarzwälder, J. P. Pekola, and D. M. Zumbühl, "Metallic Coulomb blockade thermometry down to 10 mK and below," *Rev. Sci. Instrum.* **83**, 083903 (2012).
- ¹⁷M. Palma, C. P. Scheller, D. Maradan, A. V. Feshchenko, M. Meschke, and D. M. Zumbühl, "On-and-off chip cooling of a Coulomb blockade thermometer down to 2.8 mK," *Appl. Phys. Lett.* **111**, 253105 (2017).
- ¹⁸N. Yurttagül, M. Sarsby, and A. Geresdi, "Coulomb blockade thermometry beyond the universal regime," *J. Low Temp. Phys.* **204**, 143–162 (2021).
- ¹⁹D. I. Bradley, M. Človečko, S. N. Fisher, D. Garg, E. Guise, R. P. Haley, O. Kolosov, G. R. Pickett, V. Tsepelin, D. Schmoranzler, and L. Skrbek, "Crossover from hydrodynamic to acoustic drag on quartz tuning forks in normal and superfluid ^4He ," *Phys. Rev. B* **85**, 014501 (2012).
- ²⁰S. L. Ahlstrom, D. I. Bradley, M. Človečko, S. N. Fisher, A. M. Guénault, E. A. Guise, R. P. Haley, O. Kolosov, P. V. E. McClintock, G. R. Pickett, M. Poole, V. Tsepelin, and A. J. Woods, "Frequency-dependent drag from quantum turbulence produced by quartz tuning forks in superfluid ^4He ," *Phys. Rev. B* **89**, 014515 (2014).
- ²¹M. J. Jackson, O. Kolosov, D. Schmoranzler, L. Skrbek, V. Tsepelin, and A. J. Woods, "Measurements of vortex line density generated by a quartz tuning fork in superfluid ^4He ," *J. Low Temp. Phys.* **183**, 208–214 (2015).
- ²²D. O. Clubb, O. V. L. Buu, R. M. Bowley, R. Nyman, and J. R. Owers-Bradley, "Quartz tuning fork viscometers for helium liquids," *J. Low Temp. Phys.* **136**, 1–13 (2004).
- ²³N. Samkharadze, A. Kumar, M. J. Manfra, L. N. Pfeiffer, K. W. West, and G. A. Csáthy, "Integrated electronic transport and thermometry at milliKelvin temperatures and in strong magnetic fields," *Rev. Sci. Instrum.* **82**, 053902 (2011).
- ²⁴R. Blaauwgeers, M. Blazkova, M. Človečko, V. B. Eltsov, R. de Graaf, J. Hosio, M. Krusius, D. Schmoranzler, W. Schoepe, L. Skrbek, P. Skyba, R. E. Solntsev, and D. E. Zmeev, "Quartz tuning fork: Thermometer, pressure- and viscometer for helium liquids," *J. Low Temp. Phys.* **146**, 537–562 (2007).
- ²⁵D. I. Bradley, M. Človečko, S. N. Fisher, D. Garg, A. M. Guénault, E. Guise, R. P. Haley, G. R. Pickett, M. Poole, and V. Tsepelin, "Thermometry in normal liquid ^3He using a quartz tuning fork viscometer," *J. Low Temp. Phys.* **171**, 750–756 (2012).
- ²⁶D. Lotnyk, A. Eyal, N. Zhelev, T. S. Abhilash, E. N. Smith, M. Terilli, J. Wilson, E. Mueller, D. Einzel, J. Saunders, and J. M. Parpia, "Thermal transport of helium-3 in a strongly confining channel," *Nat. Commun.* **11**, 4843 (2020).
- ²⁷M. Človečko, E. Gažo, M. Kupka, M. Skyba, and P. Skyba, "High quality tuning forks in superfluid He-3-B below 200 μK ," *J. Low Temp. Phys.* **162**, 669–677 (2011).
- ²⁸M. Človečko and P. Skyba, "Quartz tuning fork—A potential low temperature thermometer in high magnetic fields," *Appl. Phys. Lett.* **115**, 193507 (2019).
- ²⁹K. A. Modic, M. D. Bachmann, B. J. Ramshaw, F. Arnold, K. R. Shirer, A. Estry, J. B. Betts, N. J. Ghimire, E. D. Bauer, M. Schmidt, M. Baenitz, E. Svanidze, R. D. McDonald, A. Shekhter, and P. J. W. Moll, "Resonant torsion magnetometry in anisotropic quantum materials," *Nat. Commun.* **9**, 3975 (2018).
- ³⁰K. A. Modic, R. D. McDonald, J. P. C. Ruff, M. D. Bachmann, Y. Lai, J. C. Palmstrom, D. Graf, M. K. Chan, F. F. Balakirev, J. B. Betts, G. S. Boebinger, M. Schmidt, M. J. Lawler, D. A. Sokolov, P. J. W. Moll, B. J. Ramshaw, and A. Shekhter, "Scale-invariant magnetic anisotropy in RuCl_3 at high magnetic fields," *Nat. Phys.* **17**, 240–244 (2020).
- ³¹D. R. Brumley, M. Willcox, and J. E. Sader, "Oscillation of cylinders of rectangular cross section immersed in fluid," *Phys. Fluids* **22**, 052001 (2010).
- ³²H. H. Jensen, H. Smith, P. Wolfle, K. Nagai, and T. M. Bisgaard, "Boundary effects in fluid flow. Application to quantum liquids," *J. Low Temp. Phys.* **41**, 473–519 (1980).
- ³³M. Zhang, D. Chen, X. He, and X. Wang, "A hydrodynamic model for measuring fluid density and viscosity by using quartz tuning forks," *Sensors* **20**, 198 (2019).
- ³⁴M. T. Noble, S. L. Ahlstrom, D. I. Bradley, E. A. Guise, R. P. Haley, S. Kafanov, G. R. Pickett, M. Poole, R. Schanen, T. Wilcox, A. J. Woods, D. E. Zmeev, and V. Tsepelin, "Producing and imaging quantum turbulence via pair-breaking in superfluid $^3\text{He-B}$," *Phys. Rev. B* **105**, 174515 (2022).
- ³⁵D. S. Greywall, " ^3He specific heat and thermometry at millikelvin temperatures," *Phys. Rev. B* **33**, 7520–7538 (1986).
- ³⁶C. B. Winkelmann, E. Collin, Y. M. Bunkov, and H. Godfrin, "Vibrating wire thermometry in superfluid ^3He ," *J. Low Temp. Phys.* **135**, 3–14 (2004).
- ³⁷D. L. Martin, "Specific heat of copper, silver, and gold below 30°K," *Phys. Rev. B* **8**, 5357–5360 (1973).
- ³⁸J. Pollanen, H. Choi, J. P. Davis, B. T. Rolfs, and W. P. Halperin, "Low temperature thermal resistance for a new design of silver sinter heat exchanger," *J. Phys.: Conf. Ser.* **150**, 012037 (2009).